Journal of the Meteorological Society of Japan, Vol. 77, No. 1, pp. 117–133, 1999

A Measurement of Sea Ice Albedo over the Southwestern Okhotsk Sea

By Takenobu Toyota

Institute of Low Temperature Science, Hokkaido University, Sapporo 060-0819, Japan

Jinro Ukita

National Space Development Agency of Japan

Kay I. Ohshima, Masaaki Wakatsuchi

Institute of Low Temperature Science, Hokkaido University, Sapporo 060-0819, Japan

and

Ken'ichiro Muramoto

Faculty of Engineering, Kanazawa University, Kanazawa 920-0000, Japan

(Manuscript received 25 March 1998, in revised form 28 November 1998)

Abstract

In order to estimate sea ice albedo around the marginal sea ice zone of the southwestern Okhotsk Sea, we conducted the measurement of albedo aboard the ice breaker *Soya* in early February of 1996 and 1997. Using upward and downward looking pyranometers mounted at the bow of the ship, we obtained albedo data. We also measured ice concentration and thickness quantitatively by a video analysis. The observations show a good correlation between albedo and ice concentration. From a linear regression, sea ice albedo (ice concentration = 100 %) is estimated to be 0.64 ± 0.03 at the 95 % confidence level. The developed snow grains on sea ice due to sea water and/or solar radiation may be responsible for this somewhat lower value, compared with that over the snow-covered land fast ice in the polar region. Deviations of the observed values from this regression have a statistically significant correlation with solar zenith cosine at the 99 % level, and with ice thickness at the 95 % level. The linear regression formula which predicts albedo is also derived as the variables of ice concentration and solar zenith cosine. Although the regression coefficients are both statistically significant, the coefficient of ice concentration is much more significant in this formula than that of solar zenith cosine. The deviation of the observed albedo from this regression seems to be mainly caused by ice surface conditions rather than by ice thickness or cloud amount. All these results suggest that snow cover on sea ice plays an important role in determining the surface albedo.

We also did albedo observations of dark nilas with snow-free surface, they were estimated as 0.10 and 0.12 for ice thickness of 1 to 1.5 cm and 2 to 3 cm, respectively.

1. Introduction

The potential importance of sea ice albedo to climate system has been pointed out from model studies (*e.g.*, Shine and Henderson-Sellers (1985), Ingram *et al.* (1989)). Especially for marginal and seasonal ice zones in the southern Okhotsk Sea, sea ice albedo is expected to be a significant parameter since solar radiation is abundant even in mid winter, and its estimation is required. It may be possible to theoretically estimate sea ice albedo for specular sea ice. However, since sea ice generally has varied shapes and its surface conditions are highly complicated, theoretical estimation of sea ice albedo is almost impossible. Therefore, it is necessary to estimate it from observation.

The values of sea ice albedo have been reported from observation mainly in the polar regions (*e.g.*,

Corresponding author: Takenobu Toyota, Institute of Low Temperature Science, Hokkaido Univ., Sapporo 060-0819, Japan.

Grenfell and Maykut (1977), Grenfell and Perovich (1984), Perovich (1994), Schlosser (1988), Allison *et al.* (1993)). Around the Okhotsk Sea, albedo measurements have been carried out on the Saroma Lagoon, located at the northeastern part of Hokkaido, by Ishikawa and Kobayashi (1984).

However, most of these studies have focused on land fast ice near the shore, mostly because of observational difficulty. Although Allison *et al.* (1993) estimated sea ice albedo in the pack ice region of the Antarctic Ocean, their values were based on visually determined ice concentration with a priori set of albedo values for various surface conditions. Andreas and Makshtas (1985) have measured the incident and reflected short wave radiation over the pack ice region in the Antarctic for heat budget calculation, with little attention being paid to the value of sea ice albedo.

Thus there seems yet to be no direct measurement of sea ice albedo for pack ice regions with varying ice conditions. Given a large extent of areas with such conditions (*i.e.*, marginal and seasonal ice zones), it is important to estimate sea ice albedo from in-situ observation.

During 3 to 5 February 1996 and 2 to 9 February 1997, we carried out ice and oceanographic observations aboard an ice breaker *Soya* in the southwestern part of the Okhotsk Sea (Fig. 1) as one of the collaborative observations with the Marine Safety Agency. In these cruises, we have taken direct measurements of both surface albedo and ice conditions, in particular ice concentration and thickness.

Surface albedo data were continuously obtained from two pyranometers mounted at the bow of the ship. Each pyranometer was looking upward and downward, thus recording incident and reflected radiation. In order to check the effect of the ship shadow, a ship turning experiment was also carried out under a clear sky condition. We examined ice conditions with a set of video cameras which were looking at the front view from the mast of the ship, and the downward view from the side of the ship; the former and the latter gave a quantitative estimate for ice concentration and thickness, respectively.

In addition to ice conditions, solar altitude will be taken into account to estimate sea ice albedo. The major purpose of this study is to quantitatively estimate sea ice albedo, which will be useful to calculate heat budgets in the marginal sea ice regions and to show how much effect ice conditions and solar altitude have on sea ice albedo. Our interest here is the estimation of representative sea ice albedo over relatively large areas (more than one kilometer), rather than an exact measurement at a limited spot. According to Warren (1982), snow albedo is also affected by snow grains and cloud cover. Since most of the ice floes over the observation area were covered with snow, these effects seem significant. Although

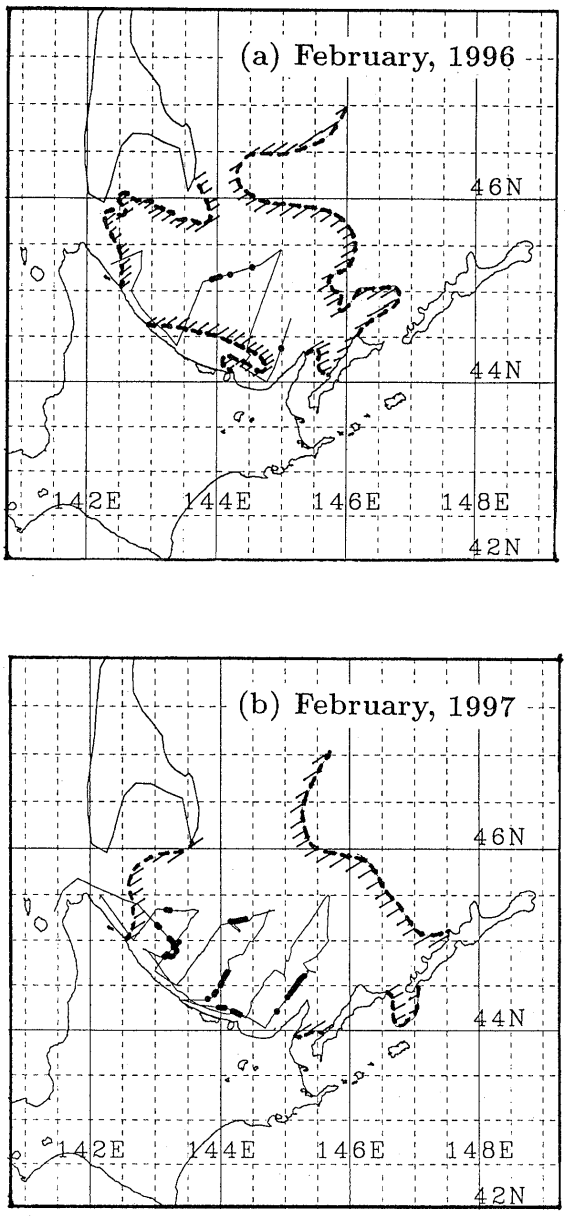

Fig. 1. Geographical map of the southwestern Okhotsk Sea with the locations of the samples used for analysis (black circles) and the ship tracks (thin line). ////// : Ice area. ((a): February 2, 1996 and (b): February 7, 1997)

we could not take the successive data of snow grains and cloud cover, several snow samples on sea ice were taken and cloud amount was observed visually at hourly intervals during the cruise. We also will discuss the effect of these factors on the basis of the data.

This paper is organized as follows: In Section 2, we will describe the ice conditions during the observation period and the method for measuring albedo and ice conditions, and then discuss the measurement error and compare the observation areas of ice concentration and albedo. In Section 3, we will ex-

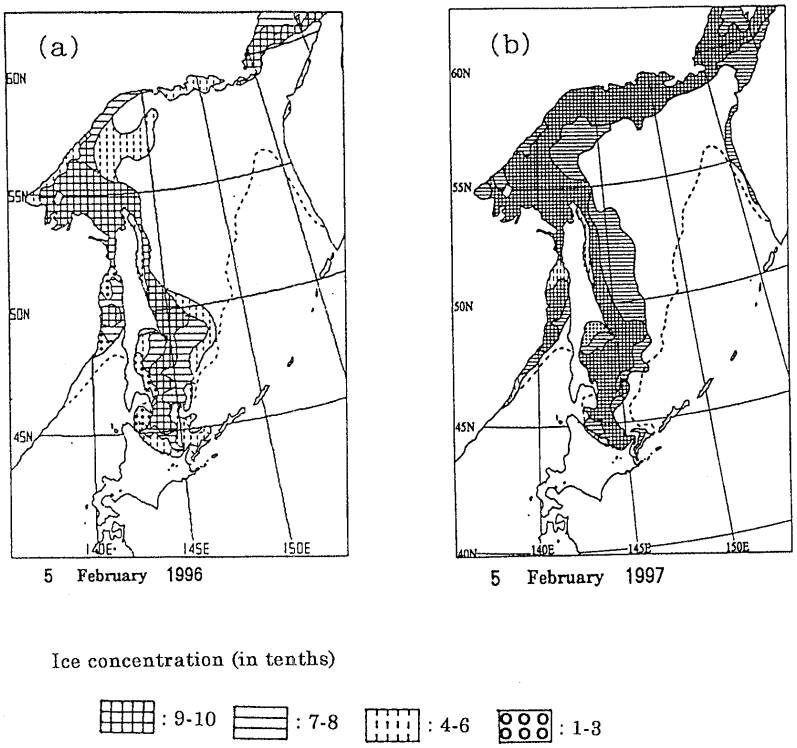

Fig. 2. Sea ice extent at the observation time in the Okhotsk Sea. Broken line means the normal averaged from 1971 to 1990. (a) February 5, 1996 (b) February 5, 1997 (adopted from Japan Meteorological Agency, 1996 and 1997).

amine the ship shadow effect from the results of a ship turning experiment. The results of analysis on the relationship between ice albedo and ice conditions will be presented in Section 4.

2. Measurement

2.1 Ice conditions

During the observation period in 1996, the weather was relatively calm with mostly clear to cloudy sky, and neither snowstorm nor big swells. The air temperature ranged from -6 to -1°C, and the wind was 4 to 10 m/s, changing from northwestern to northeastern direction. In 1997, the weather was also relatively calm. The air temperature ranged from -10 to -2°C, and the wind speed was 1 to 10 m/s. Neither snowstorms nor big swells occurred during the observation period.

Ice charts at the observation period are shown in Fig. 2 (published by Japan Meteorological Agency, 1996 and 1997). Since the data became available in 1971, the sea ice extent in the Okhotsk Sea in 1996 was record-breakingly small until early February. The sea ice extent in the southern region of the Okhotsk Sea was also below normal until late January, while it spread nearly to the norm in early February. In 1997, sea ice extended almost normally from January to February in the southern region of the Okhotsk Sea.

2.1.1 Ice concentration

During the cruise, ice concentration was monitored by a forward-looking video camera mounted at the front mast of the ship with an angle of about 10 degrees downward from level (see Fig. 3a). The video image data were then recorded on 8-mm video tapes on the video controller in the bridge room.

To process video images for ice concentration, we used a one-dimensional method developed by Muramoto *et al.* (1993). First, the continuous video images were sampled at one second intervals through an image processor to make digital data sets of individual scenes. Then, on a fixed row in each scene, we estimated the ratio of sea ice to the row length by dissecting this line into 256 segments and discriminating ice from water according to brightness (see Fig. 3b). In determining the location of the row on a video image, the further away from the ship we set it, the wider the range that can be contained for analysis but, the worse the resolution becomes. Here we selected the row so that the real width across the scene became approximately 50 m in principle, because the observed size of ice floes was mostly a few to a few tens of meters and the resolution was enough for discriminating ice from water. Finally, by averaging these successive values over a certain

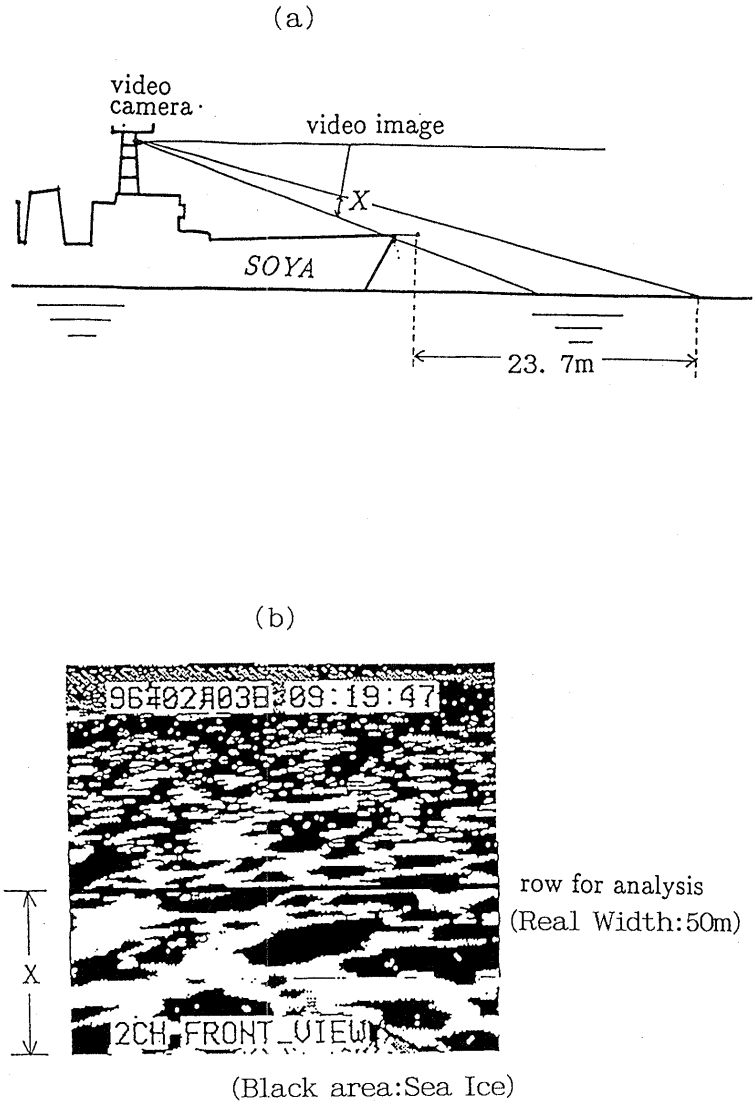

Fig. 3. Video monitoring for ice concentration. (a) Schematic picture of observation. (b) Sample of a video image. X denotes the distance from the bottom to the row used for analysis on a video image. The analyzing line is ahead of pyranometers by 23.7 m.

interval, areally mean ice concentration could be obtained along the ship track during the averaging period. We found that thusly estimated ice concentration were in good agreement with the daily operational ice charts compiled by the Marine Safety Agency.

In order to make the above analysis possible, the following conditions should be satisfied:
(1) The video image is bright enough to discriminate sea ice from water. (2) The ship is moving because successively averaged data are meaningless while the ship stops. (3) The outline of sea ice is clear enough to discriminate it from water (*i.e.*, frazil or dark ice is not appropriate). (4) The ridging of the sea ice surface is not so big as to make considerable dark shadows, (5) The direct solar radiation does not make the image saturated.

Among these constraints, (2) was the strongest. Our ship had to stop for hydrographical observation occasionally, which resulted in the relatively limited number of samples. As for (3), more or less dark ice floes which do not have clear outlines were included in many cases. Here we treated only the cases where they were not predominant for more than half of the sampling period, if any.

When the above constraints were satisfied, measurement errors seemed to be small. All the same, some errors may be contained because this method includes subjective judgment in determining the threshold of ice and water. In order to reduce the errors due to subjectivity, we repeated this measurement three times and used their averaged values for analysis.

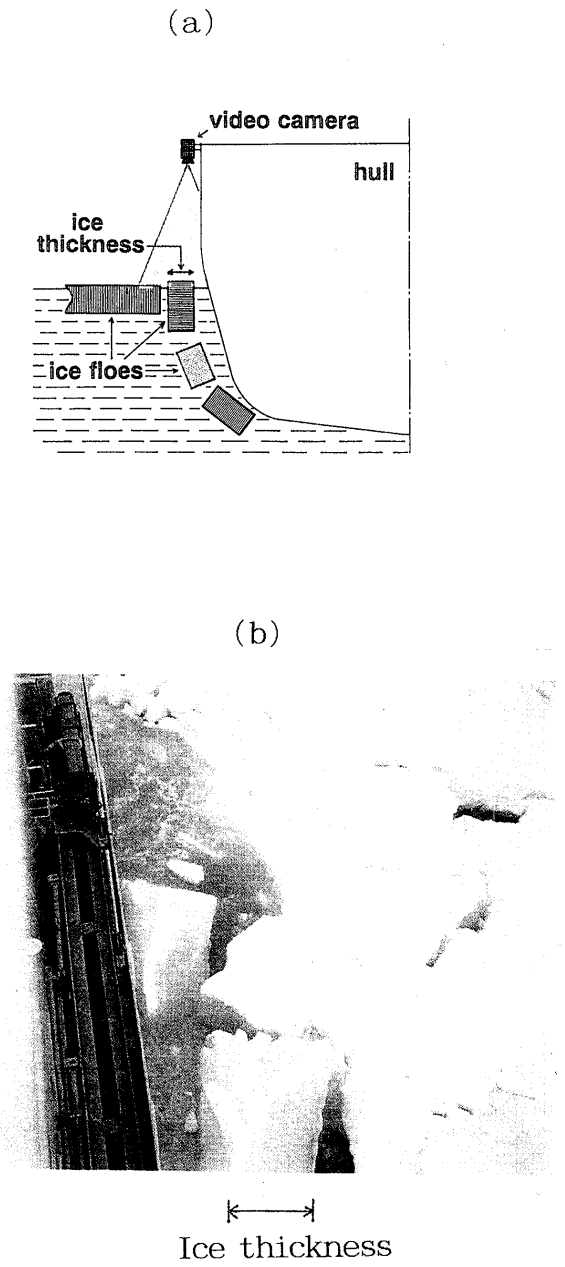

Fig. 4. Video monitoring for ice thickness analysis. (a) Schematic picture of observation (cited from Shimoda *et al.*, 1997). (b) Photograph of ice floes which were turned into side-up positions.

2.1.2 Ice thickness

Ice thickness was also monitored by a downward-looking video camera mounted at the side deck of the ship. Some ice floes which were broken at the bow were found to turn into side-up positions (Fig. 4a). For such ice floes, we measured their thicknesses manually on each video image (Fig. 4b). The method is the same as that described in Shimoda *et al.* (1997). As is shown in Fig. 4b, we refer to ice thickness as the sum of snow depth and the thickness of underlying ice.

In total, 153 and 4119 samples were obtained in 1996 and 1997, respectively. As a whole, sea ice was much thicker in 1997 than in 1996. Ice thicknesses were mostly below 30 cm and their averaged value was 18.5 cm in 1996, while it ranged from 10 cm to 150 cm and the averaged value amounted to 54.9 cm in 1997. One example of a time series of measured ice thicknesses is shown with a 10-minute averaged line in Fig. 5a. We can see from this figure that ice thickness varies on a small time scale, however, the averaged values represent the distribution of ice thicknesses as a whole. We mapped ice thickness distribution along the ship track using the averaged values (see Fig. 5b). The geographical features of ice thickness in the southern region of the Okhotsk Sea is markedly represented in this figure. Thicker ice is noticeable in the eastern part where ice floes flowed southward piling up each other from the coastal region off Sakhalin, while thinner ice is found in the western part where in-situ frozen ice is dominant.

Since there were a lot of ice floes which were thick enough for us to discriminate snow depth on video images in 1997, we also measured snow depth by difference of brightness. Although its accuracy was not high compared with that of ice thickness, the snow depth ranged from 5 to 15 cm. We did not notice marked geographical features of snow depth, as those seen with ice thickness.

2.2 Albedo

2.2.1 instruments

The pyranometers we used were S-185 type which was designed for measurement on ships by the Ishikawa Sangyou KK. They measure short wave radiation of the wavelength region 300–2800 nm from omni directions within a hemisphere with accuracy of ± 2 %, using thermopile. Their surfaces were kept horizontal by a gimbaling mechanism (see Fig. 6a). The response time is six seconds. They were calibrated by comparison with a standard instrument of Japan Meteorological Agency for the solar altitude higher than 10 degrees. Since accuracy is not guaranteed for the solar altitude less than 10 degrees, we used only data which were taken at the solar altitude greater than 10 degrees.

Installing these two pyranometers at the top and bottom of the gimbaling cylinder, we mounted these instruments at the tip of the bow with a ladder of 3 m length to avoid the shadow effect by the ship structures (see Figs. 6b,6c).

We did measurements during the period from February 3 to 5 in 1996 and from February 2 to 9 in 1997. The radiation data were accumulated successively during time intervals of 10 minutes in 1996, and one minute in 1997, and the averaged values were recorded on data loggers for every time interval. After obtaining incident and reflected short wave radiation, we calculated the averaged albedo

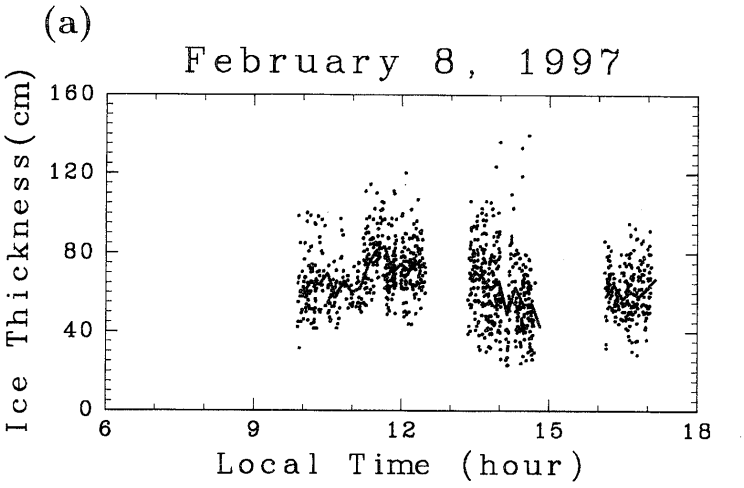

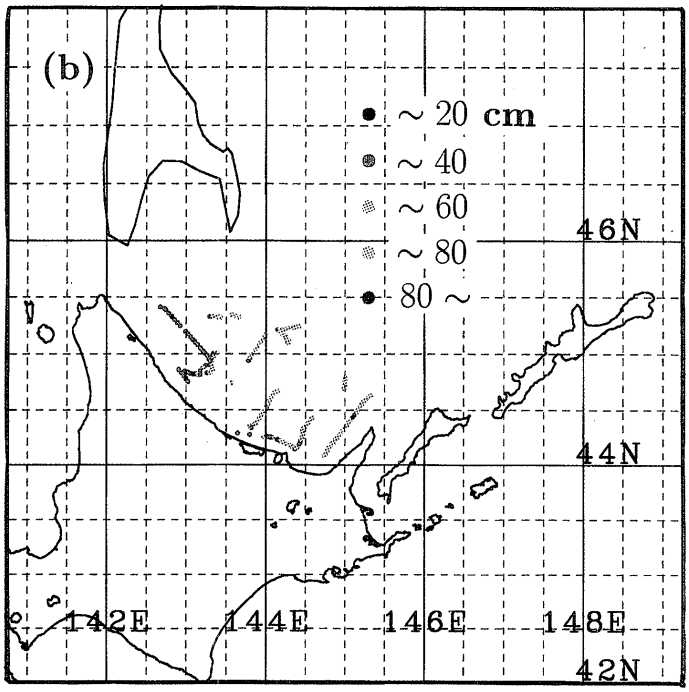

Fig. 5. Results of ice thickness analysis. (a) One example of time series of ice thickness data with a red 10-minute mean line. (b) Geographical distribution of ice thickness averaged for 10 minutes.

by taking their ratio.

2.2.2 Errors

We will discuss three kinds of errors associated with the albedo measurement. The first one is the effect of a systematic bias introduced by the shielding of the ship on upward short wave radiation (see Fig. 7). To estimate it, we calculated the upward radiant flux ($F(S)$) incident from the shielded solid angle (S) on the sphere centered on a pyranometer, assuming that radiance (I) is isotropic in direction.

$$
\begin{aligned}
F(S) &= \int\int_S I \sin\theta \cos\theta d\varphi d\theta \\
&= \int_{\theta=0}^{\theta_0} \int_{-\varphi(\theta)}^{+\varphi(\theta)} I \cos\theta \sin\theta d\varphi d\theta \\
&= I \int_0^{\theta_0} 2\varphi(\theta) \cos\theta \sin\theta d\theta \\
&\approx 4.10 * 10^{-2} I,
\end{aligned}
$$

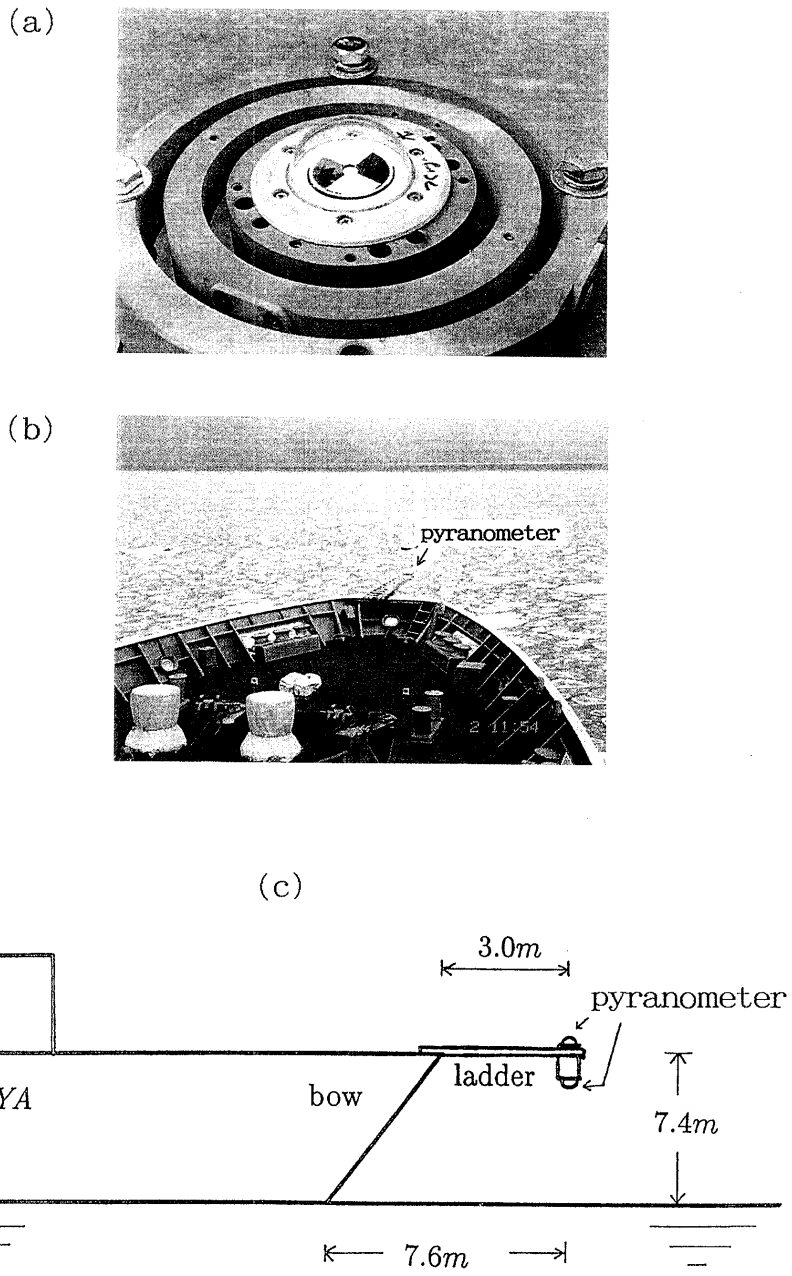

Fig. 6. Observation of short wave radiation. (a) Photograph of a pyranometer installed on gimbal. (b) Photograph of radiation measurement at the ship bow. (c) Schematic side view of arrangement.

where I, θ, and φ is radiance, incident angle, and azimuth measured from the ladder, respectively. Hence, the contribution of the shielded portion (S) to the total upward radiation (πI) is equal to $4.10 * 10^{-2} I/\pi I = 1.31 * 10^{-2}$. This implies that the effect of the ship's shielding effect is at most 1.3 % and is almost negligible. Therefore, this effect is disregarded.

The second one is the leveling error of the instruments. As for this effect, we did not take any data. However, since the ocean surface was quite calm in the ice extent during the observation period, the gimbaling mechanism seemed to function well in response to the slight vibration. For reference, during another cruise of the same ship over ice regions of the southern Okhotsk Sea in 1997, the rolling and pitching angles were both below 0.5 degree, according to Shimoda (1998, personal communication). Therefore, we regarded the leveling error as negligible.

The last error is the effect of ship shadow reflected on the ice surface. We examined it by a ship turning experiment. Through this experiment, we investigated the dependence of albedo on the solar azimuth relative to the ship head. After all, it was

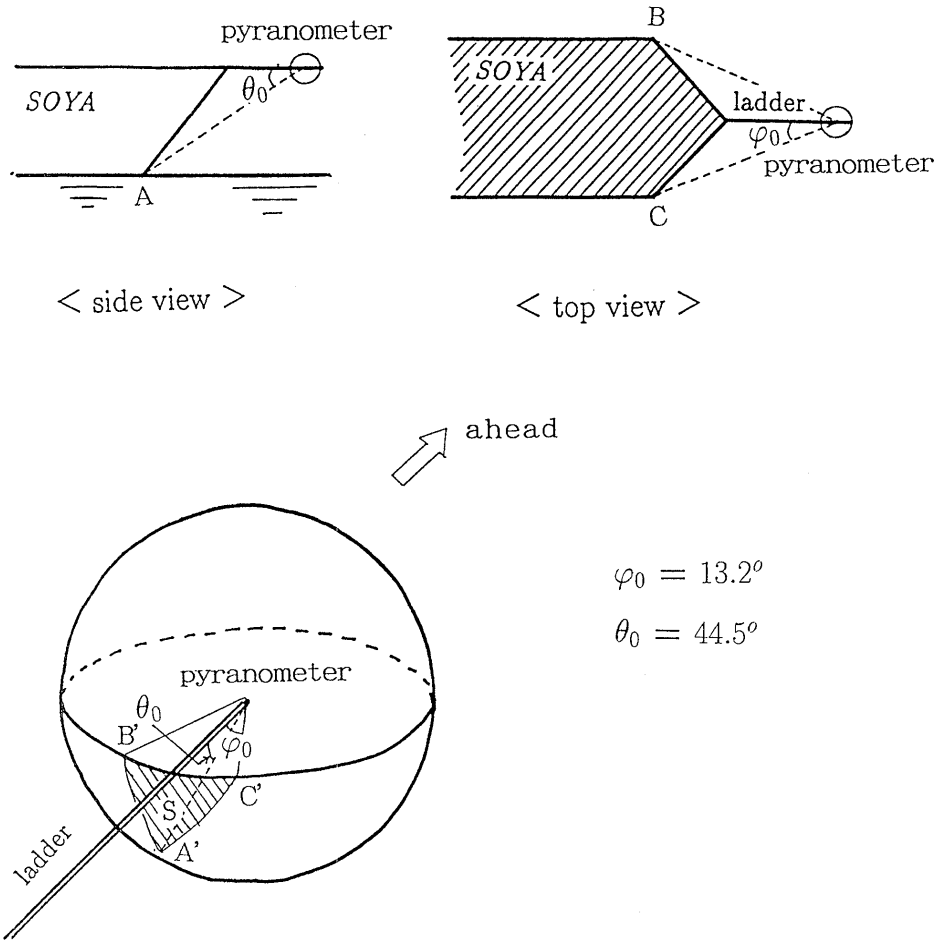

Fig. 7. Schematic pictures used for calculating the shielding effect of the ship's geometry. Slanted lines in top view denote the shielded area. A', B' and C' are the points projected to the sphere centered on a pyranometer from A, B and C, respectively.

shown that this effect should be taken into account when the sun was behind the ship. The detailed result will be shown in the next section.

2.3 Comparison of observation areas

Although the instantaneous observation area of ice concentration is different from albedo, these areas overlap as the ship moves. To discuss the relationship between ice concentration and albedo, the overlapped area should occupy a large fraction of each observation area. For this purpose, we have to take the average for an adequate period as follows: Since the sampling rate of radiation was 10 minutes in 1996, the minimum averaging period is required to be 10 minutes. Considering that the ship speed was about 5 m/s in the ice region, 10 minutes corresponds approximately to 3 km in distance. If we take averages over 3 km, the discrepancy of observation locations (= 23.7 m) (see Fig. 3a) is almost negligible.

Next, we examine the width of each observation area. If we here define *Rad. Ratio* as the ratio of the upward radiant flux ($F(\theta)$) contributed from the circle area just below the pyranometer to the total upward radiant flux ($F(\pi)$), it can be expressed as follows:

$$Rad.\ Ratio = \frac{F(\theta)}{F(\pi)} = \sin^2\theta$$

In Fig. 8, *Rad. Ratio* is shown as a function of D. Here, isotropic radiance is assumed. From this figure, it is shown that the ratio is 0.92 for $D = 50$ m, which corresponds to the real width of the row used for ice concentration analysis.

Consequently, it is considered that the observation areas of radiation and ice concentration coincide by 92 %. Given that the ice extent with similar ice conditions usually spread on the scale much more than 50 m, it is unlikely that ice concentration and albedo in the residual area (8 %) were significantly different and substantially alter the result. Therefore, we regarded the 10 minute period as sufficient

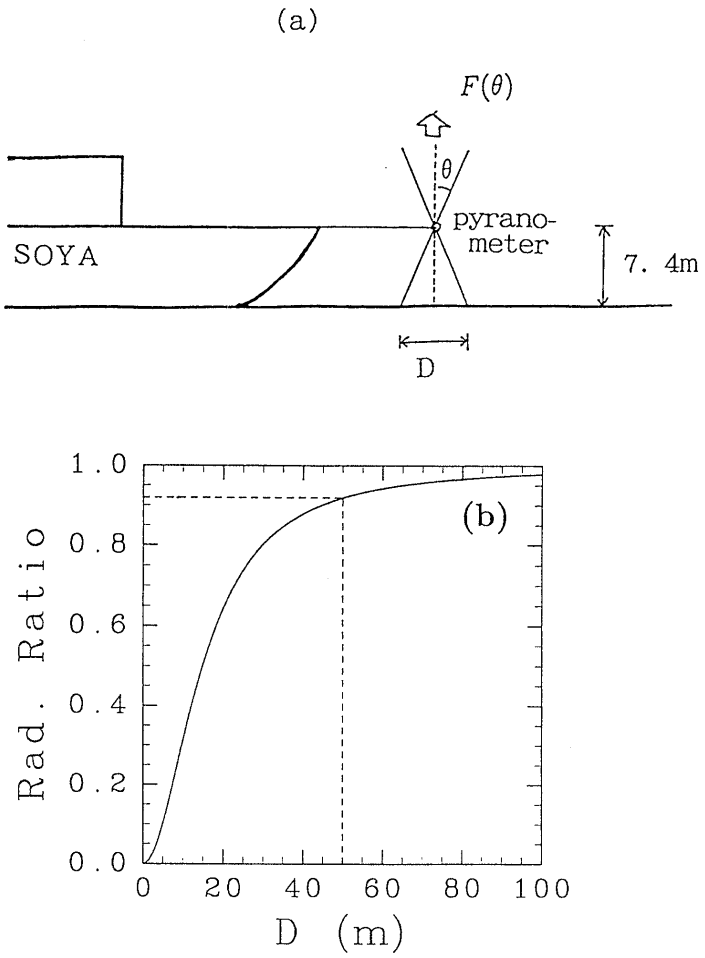

Fig. 8. Contribution of the radiation emitted from the circle area just below a pyranometer to total upward short wave radiation. (a) Geometric side view. (b) Geometrically calculated contribution as a function of the diameter (D m).

for comparison of these data. In addition, this horizontal scale of approximately 3 km matches that of our study as well. Thus 10 minutes was adopted for the averaging period.

After examining all the scenes of video images, we came up with 91 ten-minute periods (14 for 1996 and 77 for 1997) in total where both data were available for analysis.

3. Turning Experiment

Prior to an analysis of measured data, we should mention the effect of the ship shadow on the measured albedo. For this examination, we carried out a ship turning experiment around 44.9°N 143.3°E for eighteen minutes from 12h57m to 13h15m on February 9, 1997. This experiment was aimed at examining the dependence of albedo on the solar azimuth relative to the ship head by turning the ship around in a diameter of about 1 km (Fig. 9a) circle. If the shadow effect was substantial, with the increase of the ship shadow area, the decrease of the measured upward radiation would be detected. The downward irradiance seemed to be little affected by the shadow of the ship's structures because the instrument was mounted far enough from them. Therefore, if we consider only the effect of the ship shadow, the albedo measured is expected to change like a sinusoidal curve in response to the change of the relative solar azimuth, where the maximum (minimum) occurs when the sun is located ahead of (behind) the ship.

Conditions during the experiment were: weather was clear, and a definite shadow appeared as shown in Fig. 9b, solar altitude was 28 deg. at 13:00 p.m., and air temperature was about −6°C, relative humidity was 61 %, wind was 1 to 3 m/s from southeast, and ocean surface was quite calm. The ice concentration was highly variable, ranging from 40 to 90 %, which caused the variation of reflected radiation and accordingly albedo (see Figs. 10a,10b).

In order to derive the ship's shadow effect, we have to correct the effect of low albedo over open

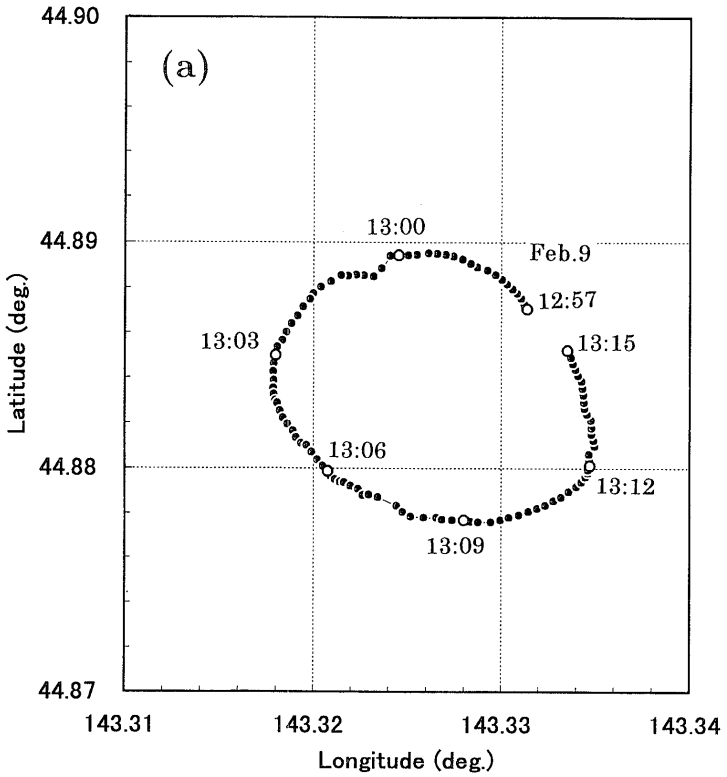

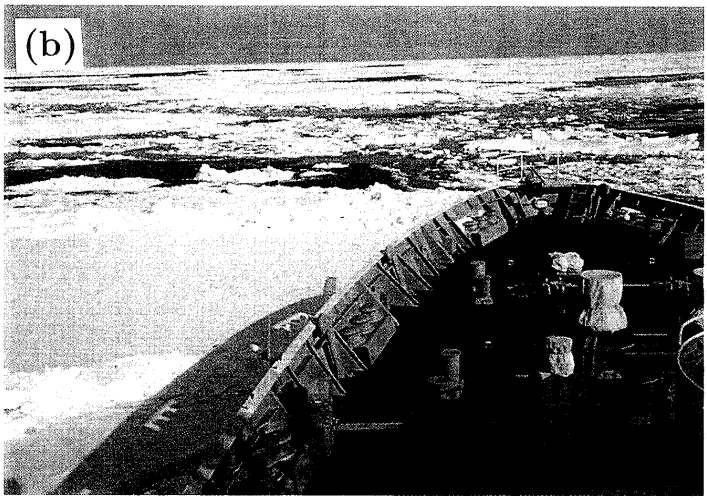

Fig. 9. Ship turning experiment conducted on February 9, 1997. (a) Ship track. The ship locations are plotted every 10 seconds. (b) Photograph of the ice conditions at the experiment.

water area. For this purpose, we examined the correlation between ice concentration and albedo, using all the 91 samples selected for analysis. As a result, it was found that albedo was highly correlated with ice concentration at more than 99 % confidence level. Therefore, we calculated the regression line to predict albedo from ice concentration and used the deviation data from this regression line instead of albedo itself to examine the shadow effect. The result is shown in Fig. 10c. In this figure, a four-dimensional fitted curve is also drawn to see the general trend more clearly. It is found from this figure that deviations became relatively lower, particularly for the relative solar azimuth beyond ± 120 degrees, when the sun was located nearly behind the ship. For example, the deviation is lower by 0.1 to 0.2 for the relative solar azimuth of 150 to 180 degrees than for that of -90 to 90 degrees.

This result indicates that the ship shadow could affect the albedo significantly when the sun was lo-

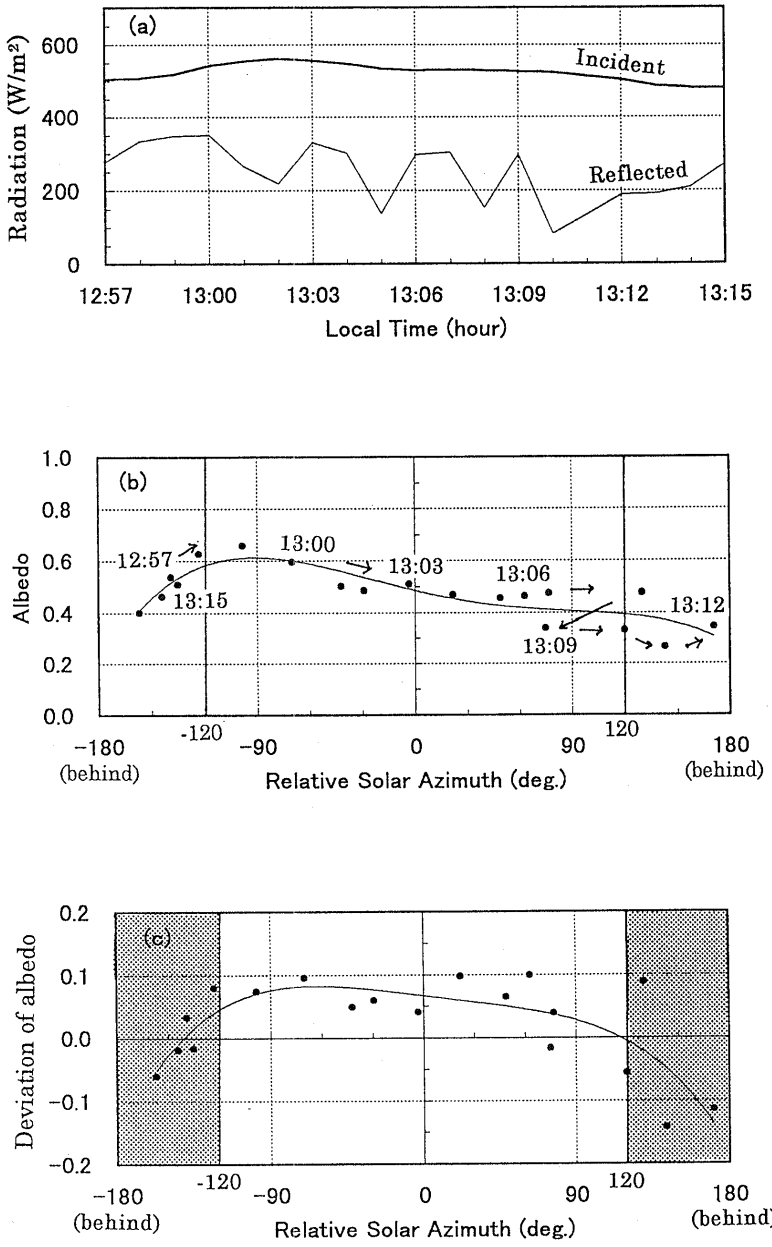

Fig. 10. Results of a ship turning experiment. (a) The time series of incident and reflected solar radiation during the experiment. (b) Plots of every minute surface albedo during the experiment (from 12h57m to 13h15m). (b) Plots of every minute deviation of albedo from the linear regression. Shaded area shows the range where the deviation is lowered than in other area. In (b) and (c), A four-dimensional fitted curve is also drawn to see the general trends.

cated nearly behind the ship under clear sky conditions. Although the decrease of albedo by ship shadow was 0.1 to 0.2 unit in the case of this experiment, this value would vary depending on the sky conditions. We consider that it would be difficult to estimate it exactly. Therefore, the data which were taken for the relative solar azimuth of greater than 120 degrees or less than −120 degrees, *i.e.*, in the case when the sun was located behind the ship, were all excluded from this analysis. After all, the number of samples used for analysis was reduced to 59 in total (6 for 1996, 53 for 1997). Their locations were plotted in Fig. 1. They all existed within the pack ice region.

Besides the above result, it should be noticed in Fig. 10a that somewhat increased incident radiation was detected, especially during the period of 13h00m to 13h06m. Because it changed smoothly and occurred only when the sun was located nearly ahead of the ship, this increase was attributed to the reflected light from the ship's structures rather than the leveling error of pyranometers. This effect

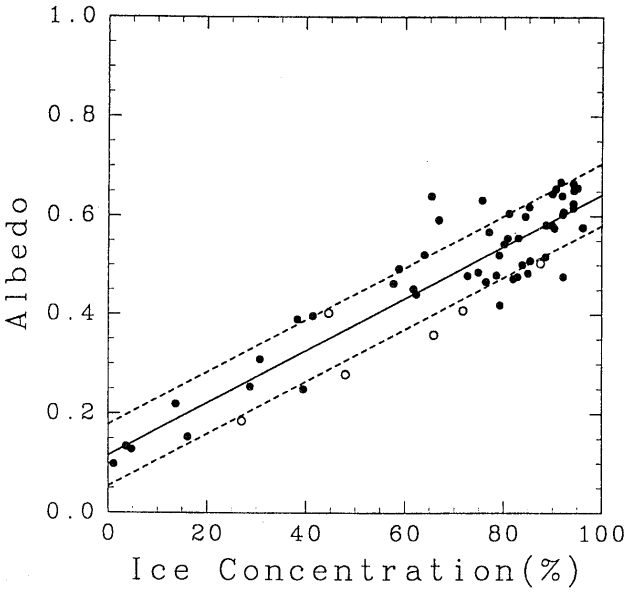

Fig. 11. Correlation between ice concentration and albedo with a regression line.White and black circles denote the data of 1996 and 1997, respectively. Two broken lines denote $\pm RMS(= 0.062)$.

caused the measured albedo to become apparently lower, resulting in somewhat lower deviation when the sun was located nearly ahead of the ship (about at 13h03m). This result implies that the measured albedo may be affected by the ship structure for the case when the sun is located nearly ahead of the ship under clear sky conditions. However, since such a case was not included in the above 59 samples, we did not take this effect into account.

4. Results

Figure 11 shows albedo as a function of ice concentration with a regression solid line. As is expected, the surface albedo for a mixed surface condition with both ice and water is linearly related to ice concentration at more than 99 % confidence level. The regression line is

$$A = 0.116 + 0.527 * \frac{c}{100}$$
$$RMS = 0.062 \qquad (1)$$

where c and A are ice concentration (%) and albedo, respectively, and RMS means root mean square which shows the difference between the observation and the prediction by the regression. Since the samples are concentrated between 60 % and 100 % ice concentration, sea ice albedo (100 % ice cover) can be estimated with significant accuracy. The regression line allows us to estimate the sea ice albedo as 0.64 ± 0.03 at the 95 % confidence level.

The sea ice albedo calculated here is somewhat higher than the value of 0.61, which was similarly estimated from a regression line of ice concentration versus albedo in a region of the Antarctic by Allison *et al.* (1993). Besides, the variation of our data from the regression line is much smaller compared with that of their data. These differences are mainly attributed to the existence of various ice types, in particular dark nilas in their data. The fact that we excluded the dark nilas from our analysis, because it was difficult to distinguish such ice from water, is likely the reason for somewhat higher albedo and smaller variations from the regression.

Although surface albedo and ice concentration were highly correlated as a whole in Fig. 11, the deviations from the regression line are also noticeable especially at high concentration. We next will consider other factors to examine the cause of these deviations.

Most of the ice floes except nilas were found to be covered with snow during the cruise, so that snow seemed to have significant effects on the surface albedo. According to Warren (1982), snow albedo is determined mainly by snow grain sizes, solar zenith angle, and cloud cover. Among these factors, it is solar zenith angle that we can obtain quantitatively with accuracy. Therefore, we focus here on the effect of the solar zenith angle among these factors. Although snow grain sizes and cloud cover were not measured successively, we took several snow samples and conducted the visual observation of cloud amount in tenths at hourly intervals. On the basis of these data, the effect of cloud amount and snow grain sizes will be discussed later.

In addition to these factors, it is known that sea ice albedo varies corresponding to ice thickness (*e.g.*, Weller, 1972). Therefore, we examined the correlation between the deviations and the 10-minute averaged total thicknesses measured by the method described in Section 2.1. When ice concentration were low, the accuracy of the ice thickness measurement decreased because it became easier for thick ice floes to flow around the ship rather than to be broken and turn into the side-up positions. For this reason, we dealt with ice thickness data only when the ice concentration was greater than 70 %. Although snow depth may also affect albedo, we did not deal with this parameter directly because of an accuracy problem. (Actually, we examined the effect of measured snow depth on the deviations of albedo for 1997 data, but significant effect could not be found.)

The individual correlation with the deviations from the regression line (1) is shown in Figs. 12a and 12b. The trends for solar zenith cosine and ice thickness, which are drawn in these figures, are both significant at the 95 % level. Therefore, we examined their effects on albedo by including them in the regression variables.

Since the correlation with solar zenith cosine is more significant (significant at the 99 % level) in

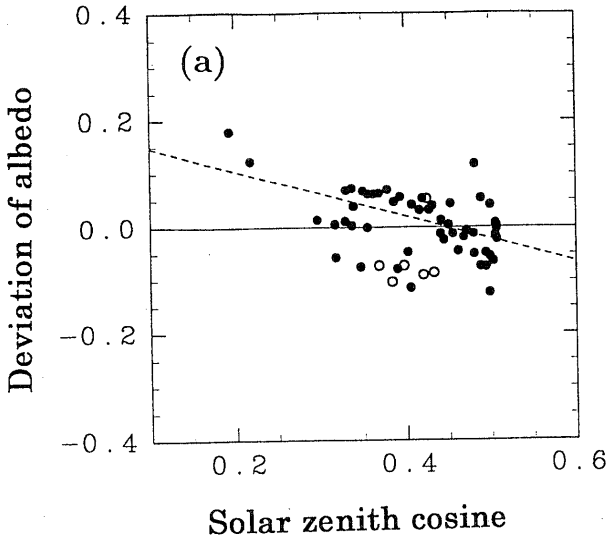

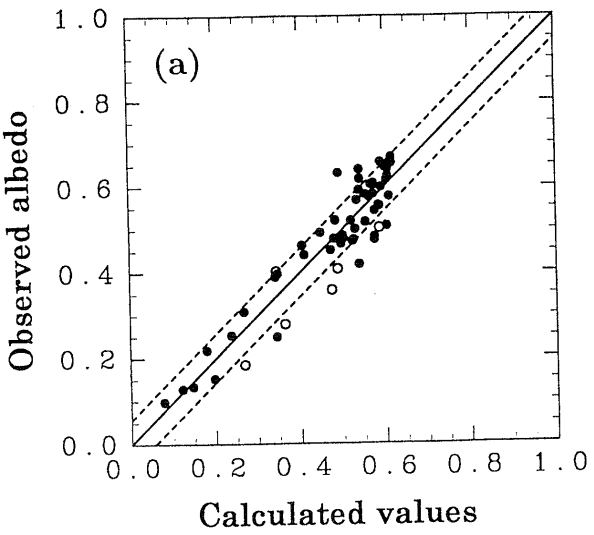

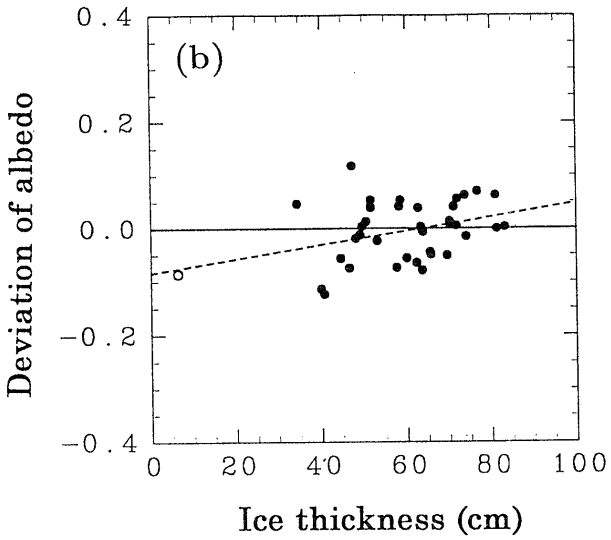

Fig. 12. Deviation of the observed albedo from the regression line in Fig. 11 as a function of (a) solar zenith cosine and (b) ice thickness. In both figures, regression lines are also drawn to see the trends.

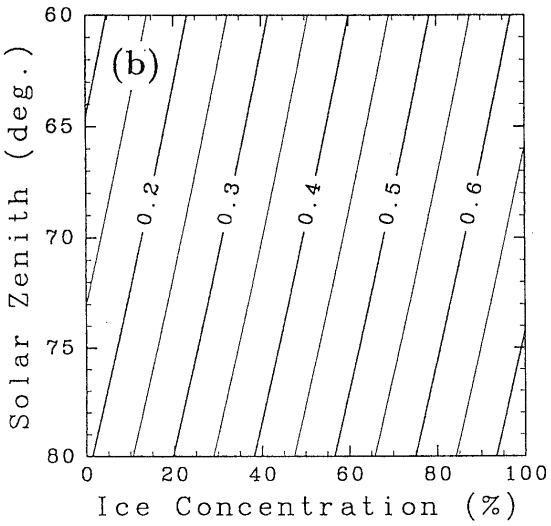

Fig. 13. Albedo calculated from ice concentration and solar zenith cosine using regression (2). (a) Correlation between observation and calculation. White and black circles are same as Fig. 11. Two broken lines denote $\pm RMS(= 0.056)$. (b) Contour map as a function of solar zenith and ice concentration.

Fig. 12 than that with ice thickness, we first derived a linear regression adding the term of solar zenith cosine. The linear regression is represented as

$$A = 0.256 + 0.543 * \frac{c}{100} - 0.364 * \cos \mu$$
$$RMS = 0.056 \qquad (2)$$

where μ is solar zenith angle. The value of RMS was somewhat reduced compared with that (=0.062) of the regression (1). The correlation between observation and calculation from this regression is shown in Fig. 13a. It is shown that the variation from the line is somewhat reduced compared with that in Fig. 11. The regression coefficients of ice concentration and solar zenith cosine are both statistically significant at the 95 % level. Figure 13b is the contour map which represents the regression (2). We see from this figure that the increase of the solar altitude by 20 degrees causes the decrease of albedo for the same ice concentration by approximately 0.1. This result is consistent with the observation of snow

albedo shown in Fig. 12 of Warren (1982). Therefore, regression (2) may possibly be close to the reality. However, the regression coefficient of ice concentration in the regression (2) is much more statistically significant than that of solar zenith cosine, and hence the dependence of albedo on solar zenith is much weaker than that of ice concentration.

Next, we will examine the effect of ice thickness which contributed weakly but statistically significantly related to albedo in Fig. 12b. We again derived the linear regression from the variables of ice concentration, solar zenith, and ice thickness. The regression line is represented as

$$A = 0.066 + 0.625 * \frac{c}{100} - 0.241 * \cos\mu + 0.109 * \frac{Hi}{100}$$
$$RMS = 0.050$$
$$(c \geq 70\ \%, N = 37) \qquad (3)$$

where Hi is ice thickness (cm). Although the value of RMS is slightly reduced again compared with that (= 0.056) of the regression (2), statistical analysis shows that the regression coefficient of ice thickness is not significant at the 95 % level. That is, the regression (3) which includes ice thickness as an additional variable, is not statistically significant, and other factor should be considered to explain the deviation of the observed values from the prediction by the regression (2). To know what caused the observed albedo to considerably deviate from the regression, we examined cloud amount data and the surface conditions.

Since cloud amount data were taken only at hourly intervals, we took out the samples in which cloud amount was observed at the same time, and plotted the deviation of the observed values from the regression (2) as a function of cloud amount. The result is shown in Fig. 14. The solar altitude (unit: degree) of each sample is also plotted. The deviation is varied even for similar solar altitude and significant dependence on cloud amount can hardly be found in this figure. Besides, for the samples which deviated from the regression by more than RMS of Fig. 13a, the cloud amount data which are estimated by interpolating from the hourly data are varied from 1 to 10. This suggests that cloud amount is not a main factor which causes the deviation.

In order to examine the effect of the surface conditions, we checked the monitored video images for the cases where the observed values deviated considerably from the regression (2). In Fig. 13a, there are six points where the observed values are greater than the predicted values by more than RMS. The investigation with the video images revealed that many relatively large ice floes (their diameters are greater than a few hundreds of meters) are found during the observation period in the five cases among six. Although ice floes of a few tens of meters in diameter are dominant in the remaining one case, the averaged ice concentration is 95 % and highly close pack ice conditions are dominant. On the other hand, there are 10 points where the observed values are less than the predicted values by more than RMS. In these cases, ice floe sizes are below a few tens of meters and thin ice with a relatively small amount of snow seems to be dominant. We consider that these features are responsible for lowering albedo. From these results, it is suggested that ice surface conditions have a more significant effect on albedo than cloud amount. In each case, surface roughnesses were occasionally found though their degrees and frequencies were varied. Such roughnesses may possibly weaken the effect of cloud cover, because they play the same role in increasing the scattered light as does cloud cover.

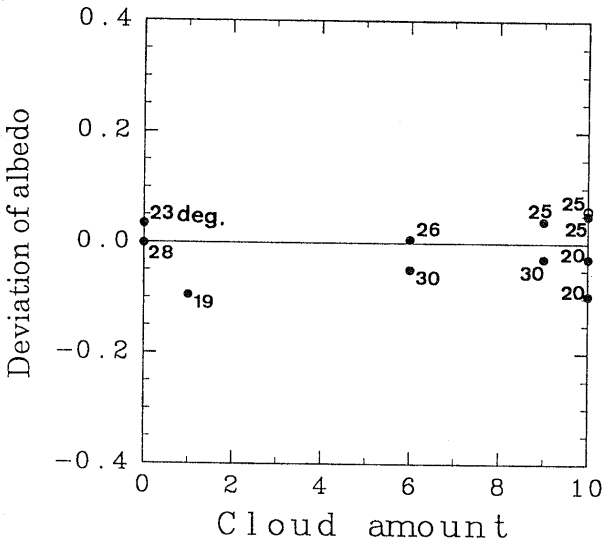

Fig. 14. Correlation between cloud amount and the deviation of observed albedo from the calculation in Fig. 13a. Only the cases in which cloud amount was also observed are shown. The numbers plotted in the figure mean solar altitude (deg.) White and black circles are same as Fig. 11.

Albedo of Dark Nilas

In the case of snow-free sea ice, we obtained albedo data for dark nilas off the Shiretoko Peninsula at 10:30 a.m. (26° Solar altitude) on February 5, 1996 and at 44.9°N 143.3°E at 01:30 p.m. (again 26° Solar altitude) on February 9, 1997 while the ship was stopped for hydrographical observations. In both cases, surrounding areas were entirely covered with nilas. The ice thicknesses, which were measured by taking samples with a net from the ship, were 1 to 1.5 cm for the former one and 2 to 3 cm for the latter one; the observed values of albedo

were 0.10 and 0.12, respectively. In the light of approximately the same solar altitudes, a slight difference may be attributed to the difference of the ice thicknesses. These albedo values were in good agreement with the earlier works. (*e.g.*, Weller (1972), Allison *et al.* (1993)).

5. Conclusions and Discussion

Sea ice albedo is an important parameter especially in the pack ice regions at low latitudes for heat budget calculation. Since it is almost impossible to theoretically estimate it for real sea ice of varied conditions, we conducted the in-situ measurements of surface albedo and ice conditions in the southwestern region of the Okhotsk Sea. From the analysis focusing on the horizontal scale of a few kilometers, it was found that the surface albedo was highly correlated with the ice concentration ($RMS = 0.062$). From the regression (1), sea ice albedo (100 % ice concentration) is estimated as 0.64±0.03 at the 95 % confidence level. The deviation from the regression line had statistically significant correlation with the solar zenith cosine at the 99 % level, and with ice thickness at the 95 % level. If we include the solar zenith cosine as an additional variable in the regression, the RMS was reduced to 0.056. Although this regression (2) is also statistically significant, the regression coefficient of ice concentration is much more significant than that of the solar zenith cosine. If we again added ice thickness to the variables of the regression, the RMS was reduced to 0.050. However, the regression coefficient of ice thickness was not statistically significant. The data which deviated considerably from regression (2) seem to be caused by surface conditions rather than ice thickness or cloud cover. From an examination of video images, it was found that albedo of less snow covered ice floes is lowered, whereas for remarkably large ice floes albedo is heightened.

In addition, we could also obtain the albedos of dark nilas with snow-free surface when the ship stopped. They were estimated to be 0.10 and 0.12 for ice thickness of 1–1.5 cm and 2–3 cm, respectively.

Among these results, we discuss two noticeable points. The first point is that the estimated sea ice albedo was somewhat lower than that of the previous studies on land fast ice covered with almost the same snow depth before melting. According to Grenfell and Perovich (1984), 0.79 is estimated for snow covered (snow depth is 8 cm) first-year ice near the shore of Alaska before melting starts. However, for the interior pack ice region, nearly the same albedo as ours is reported in the Antarctic Ocean by Andreas and Makshtas (1985). They observed surface albedo of 0.5 to 0.6 for the sea ice area with about 90 % ice concentration. Although they did not measure sea ice albedo (100 % ice concentration), this result indicates that it is 0.6 to 0.7 and is in good agreement with our estimation. Therefore, it is suggested that somewhat lower albedo may be one of the characteristics of the sea ice in the pack ice regions.

Regarding the discrepancy of albedo between pack ice and land fast ice, we at first speculated that: it is caused by difference of snow features, especially grain size between land fast ice and pack ice. For land fast ice, snow undergoes a relatively less amount of morphological processes, thus retaining fine-grained structure. On the other hand, in areas with a significant variability in ice conditions, in particular ice concentration such as a marginal ice zone, the fabric structure of a snow layer is more easily modified by sea spray and/or flooding, thus resulting in the growth of snow grains. According to Warren (1982), the snow albedo highly depends on its grain size. This may be why somewhat lower albedo was estimated in our case. This speculation is not inconsistent with the fact that considerably higher albedo than that predicted by the regression was observed where remarkably large ice floes were predominant. It is likely that the growth of snow grains on remarkably large ice floes is relatively limited because they are less influenced by sea water compared with those on small ice floes.

To confirm our speculation, we arbitrarily took 11 snow samples on small sea ice floes with a cylinder from the ship during the cruise in 1997. Grain sizes were estimated on a sampling sheet with a scale in millimeters. Salinity was measured for melted samples after the cruise. They were almost all from 0.5 to 1.0 mm in size and classified to depth hoar or granular snow. This implies that they had already grown up enough from new snow, and supports our speculation.

Salinity data were somewhat varied from less than one permil, to more than ten permil. The samples of relatively high salinity seem to have been affected mainly by sea water through sea spray and/or flooding in the snow grain growing process. In contrast, it is considered that ones with much less salinity ($\leq$ 1 psu) were affected by factors other than sea water. Considering that abundant solar radiation, and relatively high temperature even in mid winter are the characteristics of sea ice at relatively low latitude, these factors can help the growth of snow grains. Thus, it may be said that relatively low sea ice albedo is one of the features of sea ice in the southern part of the Okhotsk Sea.

The second point is that ice thickness had a weak but statistically significant effect on sea ice albedo in Fig. 12b. When we consider the fact that the optical extinction coefficients of visible wavelengths range 60 to 90 m^{-1} for snow grain sizes of 1 mm (density is 0.41 to 0.45 Mg/m^3) (Mellor, 1977) and that snow depth was 5 to 15 cm in this study, it is

unlikely that ice thickness has a direct effect on sea ice albedo. From our measurement, strong positive correlation could be seen between 10-minute averaged ice thicknesses and snow depths. Therefore, it is natural to consider that the apparent dependence of albedo on ice thickness is caused mainly by snow depth on ice floes rather than by the ice thickness below the snow. The reason why the significant effect of measured snow depth on albedo could not be found is probably due to an accuracy problem.

From all the above discussion, it is suggested that snow on sea ice floes plays an important role in determining the albedo in the marginal pack ice regions. For better understanding, further investigation on albedo and especially the characteristics of snow on ice floes will be desired in the future.

Acknowledgments

We are sincerely grateful to the crew of *P/V Soya* of Marine Safety Agency for their kind cooperation throughout the cruise. We are also indebted to N. Iwasaka, Tokyo Merchant Vessel University, for his offering of the pyranometers. Thanks are extended to H. Shimoda of Ship Research Institute, Ministry of Transport, for his technical support for the observation and analysis of video monitoring. The calculation of the solar altitude was carried out at First Regional Maritime Safety Headquarters with the help of Y. Nabae. The material needed for mounting a ladder at the ship bow was made by T. Segawa and S. Nakatsubo of Institute of Low Temperature Science. Useful discussions with N. Ishikawa are also acknowledged. Suggestions and comments from reviewers were helpful for the improvement of this paper. This study was supported partly by a special fund, Center of Excellence (COE), for scientific research and partly by the Grant-in-Aid for Scientific Research on Priority Areas (Nos. 08241201 and 09227201), from the Ministry of Education, Science, Sports and Culture of Japan.

References

Allison, I., R.E. Brandt and S.G. Warren, 1993: East Antarctic sea ice: albedo, thickness distribution, and snow cover. *J. Geophys. Res.*, **98**, 12417–12429.

Andreas, E.L. and A.P. Makshtas, 1985: Energy exchange over Antarctic sea ice in the spring. *J. Geophys. Res.*, **90**, 7199–7212.

Grenfell, T.C. and G.A. Maykut, 1977: The optical properties of ice and snow in the Arctic Basin. *J. Glaciol.*, **18**, 445–463.

Grenfell, T.C. and D.K. Perovich, 1984: Spectral albedos of sea ice and incident solar irradiance in the southern Beaufort Sea. *J. Geophys. Res.*, **89**, 3573–3580.

Ingram, W.J., C.A. Wilson and J.F.B. Mitchell, 1989: Modeling climate change: an assessment of sea ice and surface albedo feedbacks. *J. Geophys. Res.*, **94**, 8609–8622.

Ishikawa, N. and S. Kobayashi, 1984: Experimental studies of heat budget of very thin sea ice. *Seppyo*, **46**, 109–119 (in Japanese).

Japan Meteorological Agency, 1996: *The results of sea ice observation, 14 (in Japanese)*.

Japan Meteorological Agency, 1997: *The results of sea ice observation, 15 (in Japanese)*.

Mellor, M., 1977: Engineering properties of snow. *J. Glaciol.*, **19**, 15–66.

Muramoto, K., K. Matsuura and T. Endoh, 1993: Measuring sea-ice concentration and floe-size distribution by image processing. *Ann. Glaciol.*, **18**, 33–38.

Perovich, D.K., 1994: Light reflection from sea ice during the onset of melt. *J. Geophys. Res.*, **99**, 3351–3359.

Schlosser, E., 1988: Optical studies of Antarctic sea ice. *Cold Reg. Sci. and Technol.*, **15**, 289–293.

Shimoda, H., T. Endo, K. Muramoto, N. Ono, T. Takizawa, S. Ushio, T. Kawamura, K. Ohshima, 1997: Observations of sea-ice conditions in the Antarctic coastal region using ship-board video cameras. *Antarctic Record*, **41**, 355–365 (in Japanese).

Shine, K.P. and A. Henderson-Sellers, 1985: The sensitivity of a thermodynamic sea ice model to changes in surfaces albedo parameterization. *J. Geophys. Res.*, **90**, 2243–2250.

Warren, S.G., 1982: Optical properties of snow. *Rev. Geophys. Space Phys.*, **20**, 67–89.

Weller, G., 1972: Radiation flux investigation. *AIDJEX Bull.*, **14**, 28–30.

オホーツク海南西部の海氷のアルベド測定

豊田威信
（北海道大学低温科学研究所）
浮田甚郎
（宇宙開発事業団）
大島慶一郎・若土正暁
（北海道大学低温科学研究所）
村本健一郎
（金沢大学工学部）

1996年と1997年の2月上旬、オホーツク海南西部の海氷域内部において、パトロール砕氷船「そうや」に乗船してアルベドの観測を行った。アルベドは船首部に上向き、下向きの短波放射計を取付けて測定した。同時に、海氷密接度および氷厚を、ビデオ観測データの解析により定量的に評価した。水平スケール数kmを対象とした解析の結果、アルベドと海氷密接度は良い相関が見られることが分かった。回帰式をもとに、海氷のアルベド (密接度100 %) は95 %の信頼区間で0.64 ± 0.03と見積もられた。従来、極域定着氷上で測定された値よりもやや小さい値が得られたのは、低緯度海氷域内では海水や日射などの影響により、海氷上の雪粒子が成長しやすいためと推定される。観測値の回帰直線からのずれは、危険率1 %で太陽天頂角と、危険率5 % で氷厚と統計的に有意な相関が見られ、海氷密接度と太陽天頂角を変数とする重回帰式も導出された。 重回帰式において、偏回帰係数はどちらも統計的に有意であるが、アルベドは太陽天頂角に比べて海氷密接度とより強い相関関係にあることが分かった。重回帰式と観測値との差異は氷厚あるいは雲量よりも主として海氷の表面状態の違いによって生じたものと推定される。これらの結果から、海氷上の積雪が海氷域のアルベドに及ぼす影響が大きいことが示唆された。

一方、dark nilas (暗い薄氷) で覆われた海面上で停船した期間中に得られた短波放射データから、氷厚1～1.5 cm の dark nilas のアルベドは0.10、氷厚2～3 cm では0.12と見積もられた。